J Neurol (1998) 245 : 781–793

ORIGINAL COMMUNICATION

Kenzo Uchida
Hisatoshi Baba
Yasuhisa Maezawa
Shoei Furukawa
Nobuaki Furusawa
Shinichi Imura

Histological investigation of spinal cord lesions in the spinal hyperostotic mouse (*twy/twy*): morphological changes in anterior horn cells and immunoreactivity to neurotropic factors

Received: 18 August 1997
Received in revised form: 17 February 1998
Accepted: 6 March 1998

K. Uchida (✉) · H. Baba · Y. Maezawa
N. Furusawa · S. Imura
Department of Orthopaedic Surgery,
School of Medicine,
Fukui Medical University, Shimoaizuki 23,
Matsuoka, Fukui 910-1193, Japan
e-mail: baba@fmsrsa.fukui-med.ac.jp
Tel.: +81-776-61-3111, ext. 2354/2356
Fax: +81-776-61-8125

S. Furukawa
Laboratory of Molecular Biology,
Gifu Pharmaceutical University,
Mitahora-higashi, Gifu 502-0002, Japan

Abstract We examined the morphology of spinal accessory motoneurons and immunoreactivity to neurotrophins, brain-derived neurotropic factor (BDNF) and neurotrophin (NT)-3, as well as the presence of reactive astrocytosis in 70 tiptoe walking Yoshimura (twy) mice that develop calcification at C1-C2 vertebral level compressing the spinal cord. At the level of compression, the area of neuronal soma and total length of dendrites of wheat germ agglutinin-horseradish peroxidase (WGA-HRP)-labelled accessory motoneurons in the medial cell pool decreased significantly with decrement in motoneuron population, relative to the control. In contrast, at sites rostral to the compressive lesion, a significant enlargement of the neuron soma and dendritic elongation were noted, associated with increased motoneuron population and decreased transverse area of the cord at the level of compression. At this site, enhanced BDNF and NT-3 immunoreactivities were evident in the anterior horn cells. In mice with a more severe degree of compression, astrocyte-like cells showing BDNF immunoreactivity became abundant and axons in the anterior column demonstrated a marked NT-3 immunoreactivity. Our results suggest increased functional activity of anterior horn cells at levels rostral to the site of compression. We speculate that the presence of BDNF and NT-3 in neurons and astrocyte-like cells is proportionate to the severity of chronic mechanical compression and may contribute to the heterotropic neuronal reserve and survival.

Key words Spinal accessory motoneuron · Anterior horn cell · Neurotrophins · Wheat germ agglutinin-horseradish peroxidase · Tiptoe-walking Yoshimura (twy) mouse

Introduction

Reductions in the transverse area of the cervical spinal cord below 55–75% of the normal value by compressive lesions may be associated with neurological deficits. Such lesions may occur in a variety of diseases such as spondylosis, ossified posterior longitudinal ligament or herniated intervertebral discs [7, 23, 31]. We have previously documented that a 40–50% reduction in the transverse area of the cervical cord represents the critical threshold for favourable post-operative neurological recovery [5, 6]. Other studies have shown that chronic compression of the spinal cord results in atrophy and loss of anterior horn cells associated with irreversible spinal cord damage [2, 23, 28, 31]. Clinically, however, even in cases with severe compression detected on radiological examination, decompression may result in favourable recovery from a profound paresis. This unexpected outcome may be explained by the survival of a group of motoneurons even in the presence of considerable mechanical compression. Furthermore, morphological changes in the compressed

cervical cord do not necessarily predict acute development of paralysis [5, 6].

Using the tiptoe-walking Yoshimura (twy) mouse, a unique model of spinal cord compression, we recently reported a progressive decline in the number of anterior horn cells when the transverse area of the cord decreased to < 70% of the control, but there was no further decline if the area of the cord was < 50% [4]. We also demonstrated that a number of accessory motoneurons that were unaffected by external compression translocated to a site rostral to the compressive lesion [7].

In order to elucidate the mechanisms of neuronal reserve and survival of anterior horn cells, we examined morphological changes in spinal accessory motoneurons of the twy mouse using wheat germ agglutinin (WGA)-horseradish peroxidase (HRP)-labelled neurons. In the presence of a variable degree of mechanical compression, we also determined the topographic localisation of expression of brain-derived neurotropic factor (BDNF) and neurotrophin (NT)-3, which have been used as markers of motoneuron survival and neuronal plasticity [20, 37, 42]. We also determined the location of glial fibrillary acidic protein (GFAP), a marker for reactive astrocytosis [14].

Materials and methods

Experimental animals

The present series of experiments was conducted in 70 twy mice (Central Institute for Experimental Animals, Kawasaki, Japan) aged 20 weeks with an average body weight of 28.5, 5.8 g (mean, standard deviation). Mutant twy mice (*twy/twy*) were maintained by brother-sister mating of heterozygous Institute of Cancer Research (ICR) mice (*+/twy*). The disorder is inherited as an autosomal recessive condition [4, 7], and the homozygous hyperostotic mouse is identified by a characteristic tip-toe walking at 3 weeks of age, but no congenital neurological abnormalities are present. The mouse exhibits spontaneous calcified deposits posteriorly at the C1-C2 vertebral level, which produce a variable degree of compression of the spinal cord between segments C2 and C3 [4, 7]. The calcified mass grows progressively with age particularly in the atlantoaxial membrane, causing profound motor paresis at 4–7 months. The twy mouse is thus an appropriate model for examining the effects of atraumatic chronic mechanical compression of the cervical cord, produced without any artificial manipulation of the cord. The presence of a large calcified deposit was confirmed in the present study by contact microradiography (Softex CMR, Softex Inc., Osaka, Japan) and histologically when the animals were killed. Eighteen ICR mice, age- and body weight-matched with the twy mice, served as controls. The experimental protocol strictly followed the Ethics Committee Guidelines for Animal Experimentation of our University (FMU).

Retrograde labelling of spinal accessory motoneurons by wheat germ agglutinin-horseradish peroxidase

For three-dimensional morphological examination of WGA-HRP-labelled accessory motoneurons, 30 twy and 6 ICR mice were studied. Following anaesthesia by intraperitoneal injection of sodium pentobarbiturate (0.05 mg/g body weight), the sternomastoid muscles were identified bilaterally under a surgical microscope. Branches of the spinal accessory nerves innervating the muscles were carefully preserved. Using a microsyringe, 1.0 µl of 2.0% WGA-HRP (Toyobo, Tokyo) dissolved in TRIS-HCl buffer (pH 8.0) was injected carefully into the middle of the superficial layer of both sternomastoid muscles. The injection site was covered with sterilised vaseline to prevent any leakage of the WGA-HRP from the injected site into the surrounding tissues. The animal was then allowed to recover from anaesthesia. Thirty-six hours later, the mouse was reanaesthetised, and the right cardiac auricle was exposed through an anterior thoracotomy and perfused with 100 ml of 4% paraformaldehyde in 0.1 M phosphate-buffered saline solution (PBS; pH 7.3) and 0.5% glutaraldehyde solution. The spinal cord segment extending between the lower medulla oblongata and C5 segment was removed en bloc immediately after perfusion through a microsurgical craniotomy and laminectomy. The neural tissue was stored in 0.1 M PBS containing 30% sucrose at 4 °C for 36 h. Serial 50 µm-thick transverse frozen sections were prepared in each mouse, and after drying at room temperature, all sections were serially mounted on glass slides and stained according to the method described by Mesulam [30]. Using this method, WGA-HRP-labelled accessory motoneurons stained dark blue with tetramethylbenzidine and counterstained with neutral red.

Three-dimensional quantitative analysis of spinal accessory motoneurons labelled by wheat germ agglutinin-horseradish peroxidase

We used the cytoarchitectonic method described by Kitamura and Sakai [24] for identifying and classifying mouse cervical cord motoneurons, as outlined in our previous publications [4, 7]. WGA-HRP-labelled accessory motoneurons are classified into three major divisions, the medial, ventrolateral and dorsolateral motoneuron cell pools. The medial cell pool (groups 1–3) of the twy mouse located between the pyramidal decussation and C3 cord segment is severely compressed by the calcified lesion. Accordingly, in the present study, quantification and morphometric analysis of the medial motoneuron cell pool were conducted on three-dimensional longitudinal mapping of the cell pool. To minimise the possible effect of mechanical artefacts and tissue shrinkage of the cord in a craniocaudal direction during histological processing [7, 28], we examined the distribution and morphology of all WGA-HRP-labelled accessory motoneurons in the medial cell pool at the cord segment between the pyramidal decussation (the segment immediately rostral to the C1 ventral root) and the level of the C3 dorsal root. All WGA-HRP-labelled accessory motoneurons in the medial cell pool on the left and right sides, with clearly identifiable perikarya and dendrites, were serially observed and counted under the microscope (Labophoto 2Y2B, Nikon, Tokyo) (Fig. 1a–d). Using a drawing tube attachment (Nikon, Tokyo), all 500 magnified neurons were traced and stored on a Macintosh Quadra 650 computer (Apple, Cupertino, Calif.) using the NIH image software (version 1.59; Ohlandorf Research, Ottawa, Ont.) for measurement of neuronal morphology. Using the methods described by Claiborne et al. [11] and Albers and Meek [1], all traced motoneurons were topographically examined with regard to arborisation of neurons (number, area of neuron soma) and dendrites (number of dendritic segments, maximum branch order, total and maximum dendritic length). The relationship between the degree of compression and these morphological changes of motoneurons was examined.

In several mice (twy, $n = 24$; ICR, $n = 5$), images of WGA-HRP-labelled accessory motoneurons were processed using the three-dimensional computerised neuronal reconstruction system [41], developed at the Department of Physiology of our University (FMU) in cooperation with Kogaku (Tokyo) and Nikon. This analysis allowed visualisation of the stereotaxic image of dendritic arborisation in an arbitrary level (z-plane) of the spinal cord. Furthermore, this system allows a direct input of the morphological data of motoneurons through the video display. The depth infor-

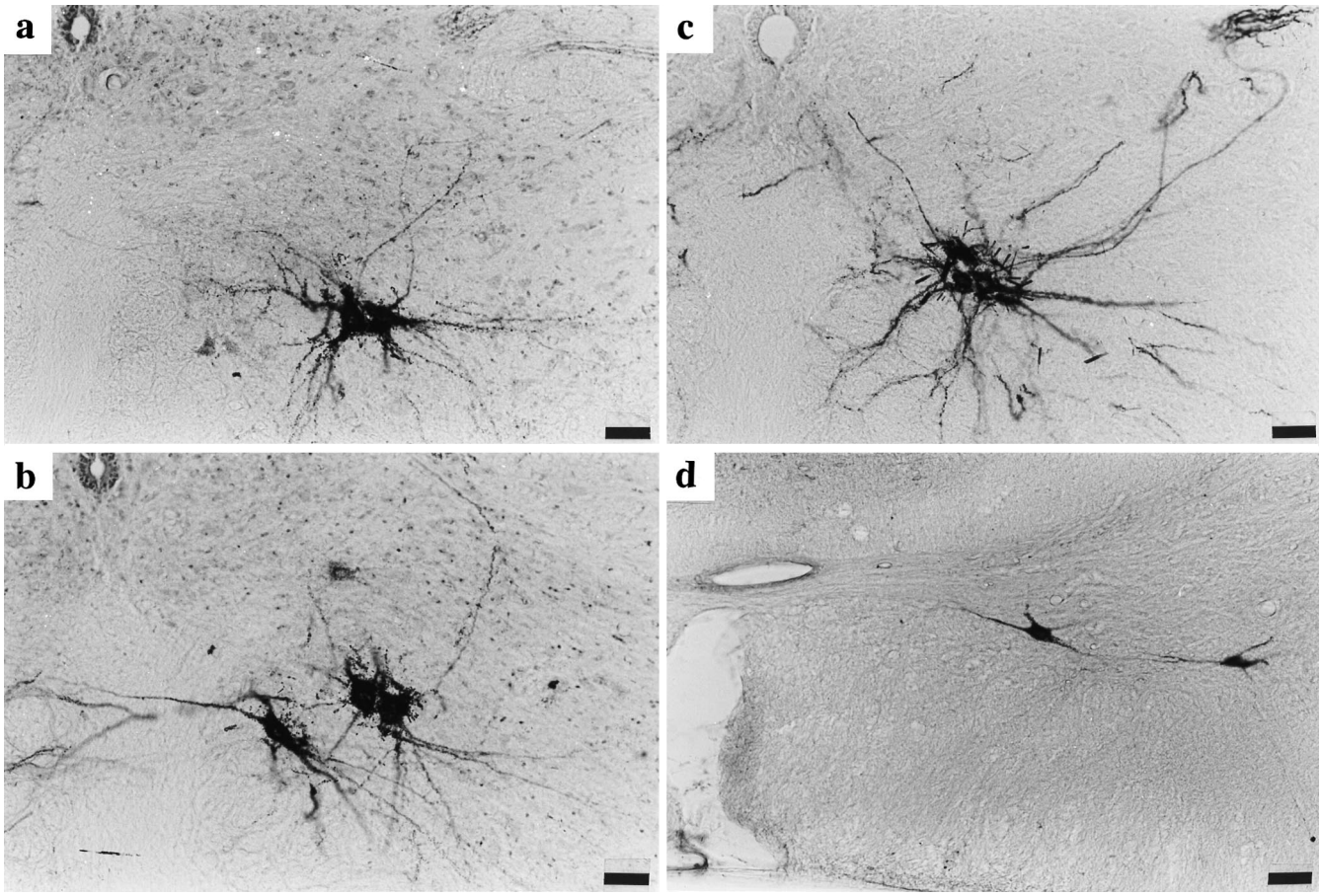

Fig. 1a–d Photomicrographs showing wheat germ agglutinin-horseradish peroxidase-labelled spinal accessory motoneurons. **a** Motoneurons at C2-C3 segments in a representative control ICR mouse; **b** site A in the twy mouse, the most rostral level; **c** site B, the level immediately rostral to the compressive lesion; **d** site C, the site of mechanical compression at C2-C3 cord segments. The *top side* in each figure represents the dorsal aspect of the cord. *Bar* 50 μm

mation (z value) is encoded by a digital micrometer attached on the stage, while the x-y plane is encoded by a digitiser.

Morphological measurements and three-dimensional computer display of the dendritic arborisation of motoneurons, and immunohistochemical studies of neurotrophins, were performed as described previously [4, 7]. For this purpose, three segments of the spinal cord were selected: site A, at the level most rostral to the C1 ventral root; site B, at the segment immediately rostral to the compression lesion between C1 ventral and C2 dorsal roots; and site C, at the site of compression between C2 and C3 dorsal roots.

Assessment of the compressed spinal cord area

The transverse area of the cervical spinal cord with the maximum compression at site C in each twy mouse was used as the index to express the magnitude of external compression. To measure the area of the compressed cervical cord, photomicrographs of all histologically stained samples magnified 50 times were processed using an x-y digitiser (Gradimate SQ-3000; Oscon, Tokyo). To compensate for a possible effect of the size of individual section and cord shrinkage during histological processing [4, 7], the transverse area of the spinal cord showing maximum compression at the level of the C1 ventral root in the twy mouse and the area of the cord at the corresponding level in the control ICR mouse were then measured. The ratio between the two transverse areas was designated as the transverse remnant area of the spinal cord [TRAS (%)] and this was again used in the present study to represent the magnitude of compression [4, 7].

Immunohistochemical processing of the spinal cord

To determine BDNF and NT-3 immunoreactivities in the cervical cord, twenty 20-week-old twy and six ICR mice were studied. After anaesthesia with intraperitoneal injection of sodium pentobarbiturate (0.05 mg/g body weight), perfusion was performed through intracardiac irrigation of 50 ml PBS (at 4 °C) followed by 100 ml of 2% paraformaldehyde in 0.1 M PBS (pH 7.6). Immediately after perfusion, the cervical cord was removed en bloc and stored in 0.1 M PBS containing 30% sucrose at 4 °C for 48 h. Serial 20 μm-thick transverse frozen sections were treated with 0.1 M TRIS-HCl buffer (pH 7.6) containing 0.3% Triton X-100 for another 24 h in order to allow reaction of the cell membrane with the antibodies. Sections were then incubated in a free-floating state with anti-BDNF V4 or anti-NT-3 V4 antibodies (each 1:30000) diluted in PBS-Triton for 48 h at 4 °C; both antibodies were recently developed by one of the authors (SF) [17] and have been confirmed to specifically express BDNF and NT-3 immunoreactivities, respectively. After blocking intrinsic peroxidase with

0.3% H_2O_2 solution, antibodies were detected by incubating the sections in TRIS-Triton containing 1 g/ml biotinylated anti-rabbit IgG antibody (ABC Elite kit, diluted 1:1000; Vector Laboratories, Burlingame, Calif.) at 4 °C for 12 h, followed by incubation in avidin-biotin-peroxidase solution (Vector Laboratories) at room temperature for 1 h. After rinsing the sections in PBS-Triton for 10 min, labelled peroxidase was visualised with 0.05 M TRIS-HCl buffer (pH 7.6) containing 0.02% 3, 3-diaminobenzidine tetrahydrochloride (DAB; Dojin Chemicals, Kumamoto, Japan), 0.6% nickel ammonium sulphate and 0.0002% H_2O_2. Hippocampus neurons were immunostained in a similar manner and used as positive controls; they were also reacted with rabbit serum IgG, then immunostained and used as negative controls [17].

To identify the presence of reactive astrocytosis, twenty 20-week-old twy and six ICR mice were studied. The cervical spinal cord was removed en bloc as described above and stored in 0.1 M PBS containing 30% sucrose at 4 °C for 24 h. Serial 20 μm-thick transverse sections treated with 0.1 M TRIS-HCl buffer (pH 7.6) were reacted with anti-GFAP antibody (GA-5; Sigma Chemicals, St. Louis, Mo.) for 12 h at 4 °C. After blocking intrinsic peroxidase with 0.3% H_2O_2 solution, the sections were incubated in avidin-biotin-peroxidase solution and allowed to react with 15 mM sodium azide (ABC Elite kit, Vector Laboratories). In order to visualise peroxidase colour reaction, sections were treated with 0.02% DAB, 0.05 M TRIS-HCl buffer at pH 7.6 and 0.0002% H_2O_2. Sections were stained with eosin and then haematoxylin for nuclear counterstaining.

Immunoblot analysis of neurotrophic factor in the spinal cord

To topographically quantify BDNF and NT-3 immunoreactivites in the cervical cord and control tissues (hippocampus), we studied ten 20-week-old twy mice with TRAS between 50–70% and ten ICR mice. The cervical cord between the most rostral site (site A) and the level distal to the compressed segment was divided into four sections. The sections were solubilised in RIPA buffer (50 mM pH 7.5 TRIS-HCL, 150 mM NaCl, 1% Triton X-100, 0.5% sodium deoxycholate, 20 μg/ml leupeptine, 1 mM PMSF), homogenised and then stored at –80 °C. Laemmli sodium dodecylsulfate buffer samples containing each protein were boiled and subjected to immunoblot analysis. Total protein (50 μg/lane) was applied to electrophoresis on sodium dodecylsulfate polyacrylamide gels (15%) and transferred onto polyvinylidene difluoride membrane (PE Applied Biosystems, Foster, Calif.) for 70 min in a semi-dry blot apparatus. The membranes were then washed twice in PBS containing 0.05% Tween 20, and subsequently reacted with anti-BDNF V4 or anti-NT-3 V4 antibody (each 1:1000) diluted for 12 h at 4 °C, followed sequentially by reaction with anti-rabbit IgG antibody and avidin-biotinylated peroxidase complex. Peroxidase activity was then visualised. To quantify the relative expression level of these neurotrophins in ICR and twy mice at each level of the spinal cord, we analysed the band densities on the photographic film with a densitometer using the NIH imaging software. Data were expressed as relative values, representing the ratio of each band density to control value in the hippocampus of the ICR mouse (%).

Statistical analysis

All measured values were expressed as mean (SD). Non-parametric Wilcoxon's signed-ranks test was used to compare the morphological data of neurons and dendrites measured at variable levels (sites A, B and C). At the level of compression (site C), these mor-

Table 1 Results of morphological measurements of neuronal soma and dendrites of the wheat germ agglutinin-horseradish peroxidase-labelled spinal accessory motoneurons in the medial cell pool of the twy and control ICR mice

	Spinal cord level			Mean (SD)	Total number (SD)
	Site A[a]	Site B[b]	Site C[c]		
twy mouse (n = 30)					
1. Neuron					
Number	34.7 (10.1)	67.9 (10.5)*	3.7 (3.2)**		106.3 (18.1)*
Area of soma (μm²)	574.0 (138.4)*	565.9 (98.9)*	324.4 (170.7)	488.0 (180.2)**	
2. Dendrite					
Number of segments	7.4 (1.1)	7.6 (1.0)	5.7 (1.1)	6.9 (1.4)	
Maximum branch order	3.0 (0.8)	3.1 (0.7)	2.8 (0.7)	3.0 (0.7)	
Total length (μm)	577.0 (142.5)*	523.8 (157.8)*	242.6 (150.8)	242.6 (150.8)	
Maximum branch length (μm)	190.6 (61.5)	183.1 (61.1)	96.9 (50.1)	156.9 (71.4)*	
ICR mouse (n = 6)					
1. Neuron					
Number	29.5 (12.1)	93.7 (10.0)	24.3 (5.5)		145.8 (17.0)
Area of soma (μm²)	529.2 (44.1)	519.4 (46.9)	526.3 (83.8)	524.8 (57.5)	
2. Dendrite					
Number of segments	7.5 (1.0)	8.3 (0.5)	6.2 (1.2)	7.3 (1.3)	
Maximum branch order	3.2 (0.8)	3.2 (0.8)	3.0 (0.9)	3.1 (0.8)	
Total length (μm)	531.8 (79.2)	418.3 (1.3)	435.6 (169.4)	461.9 (134.0)	
Maximum branch length (μm)	169.3 (28.7)	123.0 (40.7)	118.6 (38.2)	137.0 (41.4)	

* $P < 0.05$, ** $P < 0.01$ (Wilkoxon's signed-ranks test), compared with the corresponding data of ICR mice

[a] Site A: the level most rostral to C1 ventral root. Values are mean (SD)

[b] Site B: the level immediately rostral to the compression lesion between C1 ventral and C2 dorsal roots

[c] Site C: compression site between C2 and C3 dorsal roots

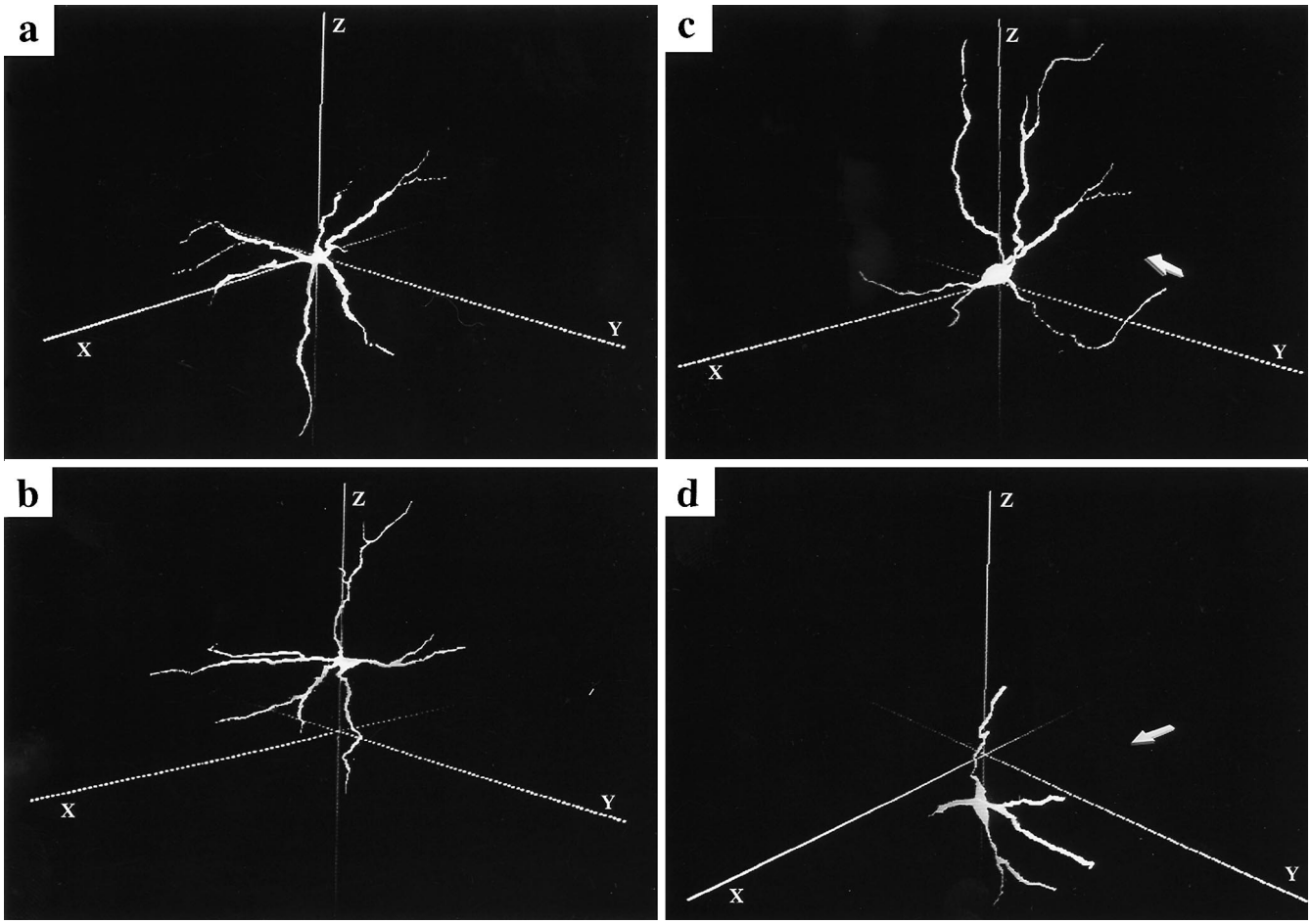

Fig. 2a–d Three-dimensional computer display of the dendritic arborisation of the wheat germ agglutinin-horseradish peroxidase-labelled spinal accessory motoneurons (*abscissa* lateral direction, *ordinate* anteroposterior direction and *z-axis* longitudinal direction). The compression force is applied in the x-y plane marked by *arrows* in **c** and **d**. **a** Motoneuron at C2-C3 segment in the control ICR mouse; **b** site A in the twy mouse, the most rostral level; **c** site B, the level immediately rostral to the compressive lesion; **d** site C, the compression level at the C2-C3 cord segments

phological parameters were statistically examined with TRAS using Pearson's correlation analysis. A P value of less than 0.05 denoted the presence of a statistically significant difference.

Results

Topographic morphology of wheat germ agglutinin-horseradish peroxidase-labelled spinal accessory motoneurons

Representative photomicrographs showing WGA-HRP-labelled accessory motoneurons in the medial cell pool of the ICR and twy mice are shown in Fig. 1, and results of morphological analysis of these motoneurons are summarised in Table 1. The average TRAS in twy mice was 44.4 (17.4)% (range 11–79). The total number of accessory motoneurons in the medial cell pool extending between the C1 and C3 cord levels in twy and ICR mice was 106.3 (18.1) and 145.8 (17.0), respectively. The number of motoneurons at site C was significantly lower in twy mice than in ICR mice ($P < 0.05$, Wilcoxon's signed-ranks test). Furthermore, at sites A and B of the twy mice, the mean area of the neuron soma was significantly larger than in ICR mice ($P < 0.05$). The proportion of the number of WGA-HRP-labelled motoneurons at site C, the compression level, to that of sites A or B, was significantly lower in twy mice than in control ICR mice ($P < 0.01$). The area of WGA-HRP-labelled motoneuron at site C was smaller in twy mice, albeit insignificantly, than the corresponding area at the same level in ICR mice.

There were no significant differences in the number of dendritic segments and the maximum branch order among different sites of the cervical spinal cord in the twy mice. No significant branching or evidence of growing dendritic cones were observed at any site in twy mice. In these mice, there was a tendency for dendrites at site C to be thicker relative to those in other sites. The total length of dendrites at sites A and B was significantly longer than in the

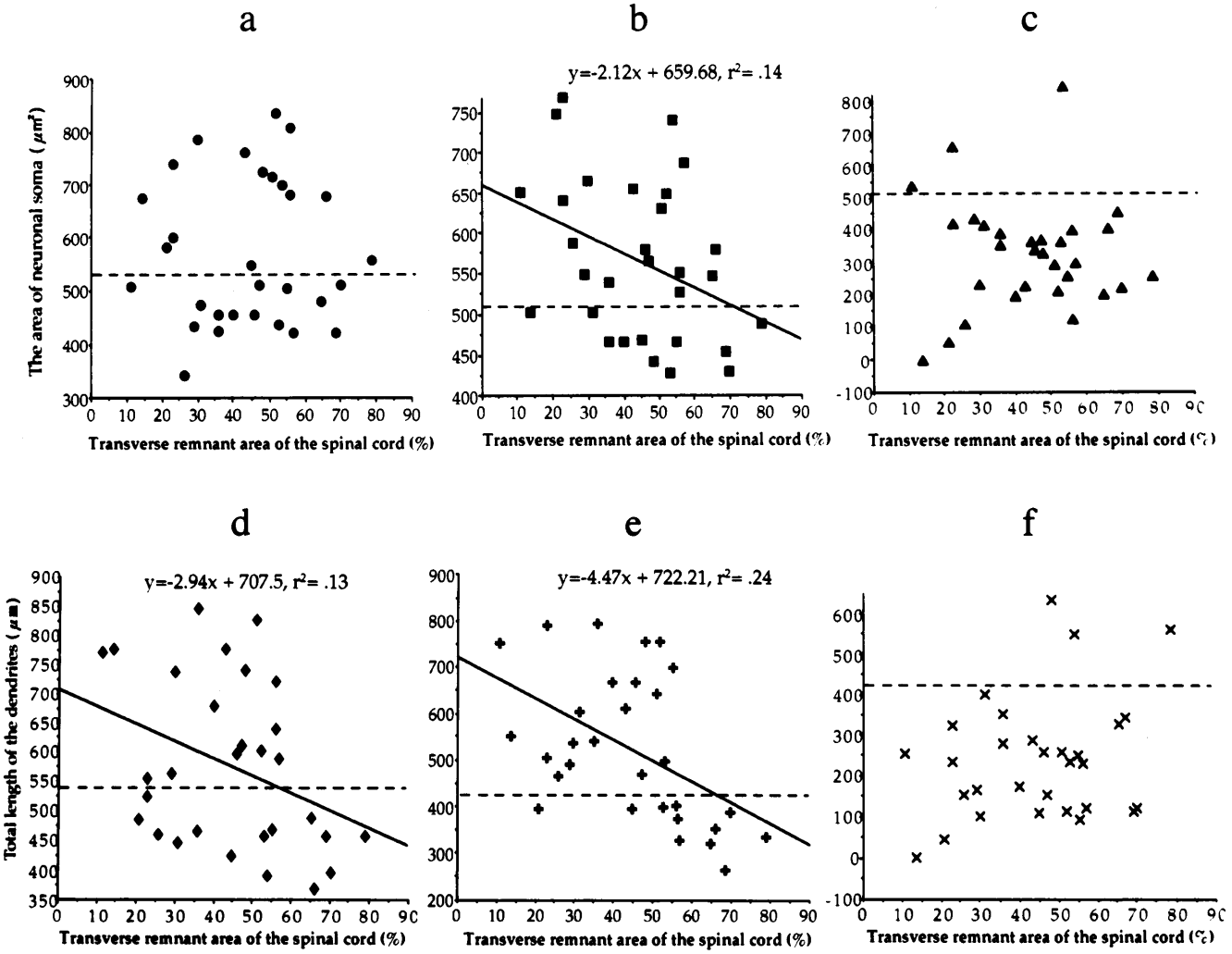

Fig. 3 Relationship between the area of neuronal soma and transverse remnant area of the spinal cord (**a–c**), and relationship between total length of the dendrites and transverse remnant area of the spinal cord (**d–f**) at three representative levels in the twy mouse. **a**, **d** Site A, the level most rostral to the C1 ventral root; **b**, **e** site B, the level immediately rostral to compression between C1 ventral and C2 dorsal roots; **c**, **f** site C, the compression site between C2 and C3 dorsal roots. *Broken lines* represent average values in control ICR mice

corresponding levels of ICR mice ($P < 0.05$). Furthermore, the maximum branch length of dendrites at site B in twy mice was significantly longer than in ICR mice ($P < 0.05$).

Three-dimensional computerised display of spinal accessory motoneurons

Representative three-dimensional computerised displays of WGA-HRP-labelled accessory motoneurons are shown in Fig. 2a–d. At site A of the twy mouse, the most rostral level, the neuronal configuration (Fig. 2b) was essentially similar to that of the control ICR mouse (Fig. 2a). At site B, the level immediately rostral to the compressive lesion, where cord compression was to some extent directed caudally and posteriorly, the elongated dendrites extended rostrally and ventrally as if the motoneuron avoided posterior compression (*arrow*, Fig. 2c). At site C in the twy mouse, in contrast to the images at sites B and A, the dendrites were shorter (Fig. 2d).

Relationship between morphology of spinal accessory motoneurons and magnitude of compression

The area of neuronal soma and total length of dendrites in twy mice at three representative levels are shown in Fig. 3a–c and Fig. 3d–f, respectively. Both parameters correlated with the magnitude of compression, i.e. TRAS, measured at site C. At site A, there was no significant correlation between the area of neuron soma and TRAS, although the area was slightly larger, but insignificantly (Fig. 3a). At site B, the level immediately rostral to the

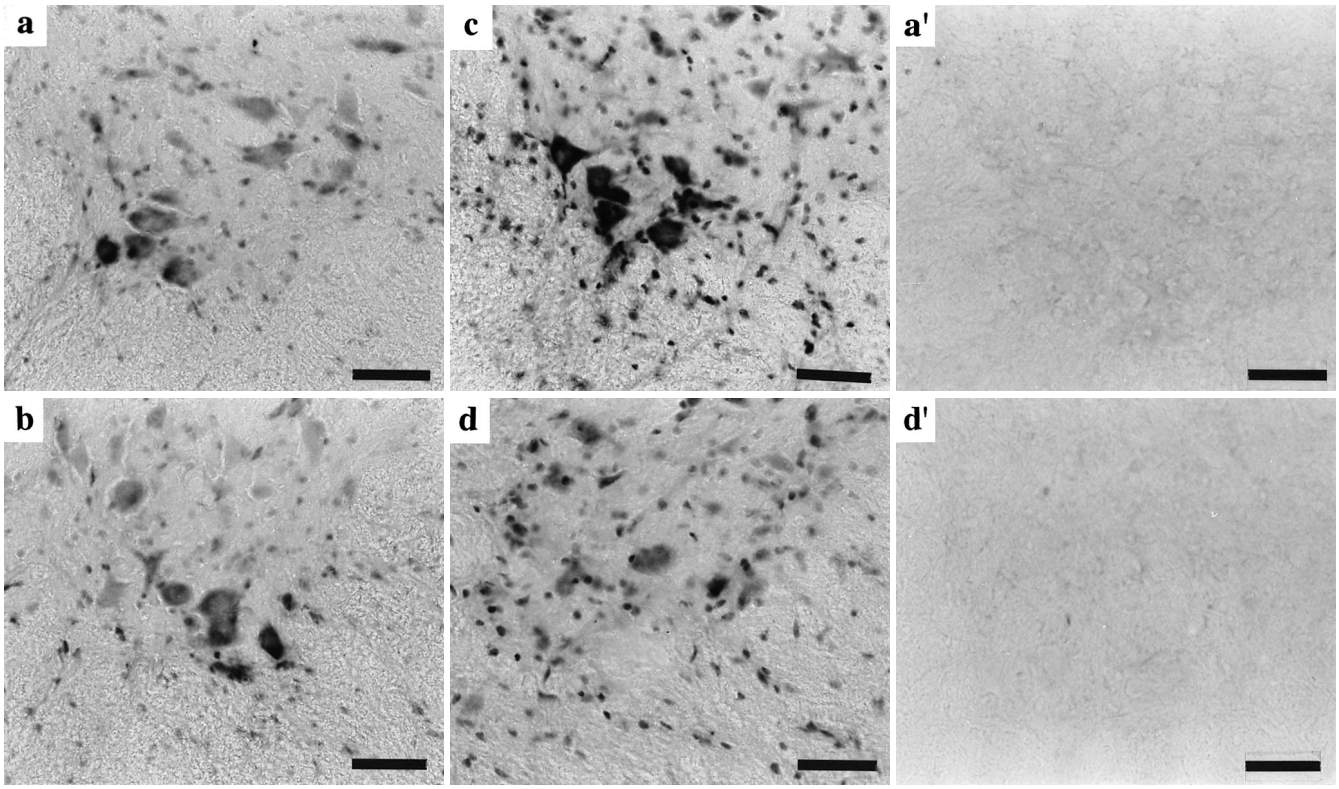

Fig. 4 Photomicrographs showing localisation of immunoreactivity of brain-derived neurotropic factor in the anterior grey horn of a representative ICR mouse (**a**) and twy mouse (**b–d**) with a transverse remnant area of 60%. **b** Site A; **c** site B; **d** site C. **a′**, **d′** Negative controls for ICR and twy mice, respectively. *Top* posterior aspect of the spinal cord. *Bar* 50 μm

site of compression, the area of neuron soma correlated significantly with TRAS (r^2 = 0.139, $P < 0.05$, Fig. 3b). Compared with the finding at site A, TRAS diminished with reductions of the somal area at site C, although the correlation between the two parameters was not significant ($P = 0.075$, Fig. 3c).

The total length of dendrites increased significantly at sites A (r^2 = 0.129, $P < 0.05$, Fig. 3d) and B (r^2 = 0.240, $P < 0.01$, Fig. 3e) as TRAS decreased. At site C, the total length of dendrites tended to decrease when TRAS diminished, albeit insignificantly ($P = 0.087$, Fig. 3f).

Localisation of brain-derived neurotropic factor immunoreactivity in the anterior grey matter and its relationship to the magnitude of compression

In control ICR mice, BDNF immunoreactivity was primarily localised in the grey matter, particularly in the anterior grey horn cells (Fig. 4a). In twy mice with TRAS values of 50–70% (n = 12), BDNF-like immunoreactivity at site A was essentially similar to that observed in ICR mice (Fig. 4b). At site B, BDNF immunoreactivity in the anterior horn cells was significantly higher than in ICR and site A in twy mice (Fig. 4c). At site C of twy mice, BDNF immunoreactivity was generally weak (Fig. 4d), although intense immunostaining was observed in a number of shrivelled motoneurons. In the presence of a more severe compression at site C (TRAS < 50%; n = 8), anterior horn cells at site B showed more significant BDNF immunoreactivity compared with that at site C of twy mice and at site B of those animals with TRAS = 50–70% as well as the corresponding level of control mice. In addition, more labelled non-neuronal astroglia- and microglia-like cells were detected at sites B and C.

Localisation of neurotrophin-3 immunoreactivity in the anterior grey horn and its relationship to the magnitude of compression

In ICR mice, the anterior horn cells were clearly stained with anti-NT-3 V4 antibody, although their nuclei were spared (Fig. 5a). In twy mice (TRAS = 50–70%), NT-3 immunoreactivity was enhanced in the anterior horn cells of site A (Fig. 5b) relative to the same area in ICR mice. Similarly, at site B, immunostaining for NT-3 V4 antibody was significant in the anterior horn cells, with enhanced immunoreactivity in the neuron soma and dendrites (Fig. 5c) compared with those seen at site A in twy and ICR mice. On the other hand, NT-3 immunoreactivity tended to diminish in the seemingly atrophic anterior horn cells at

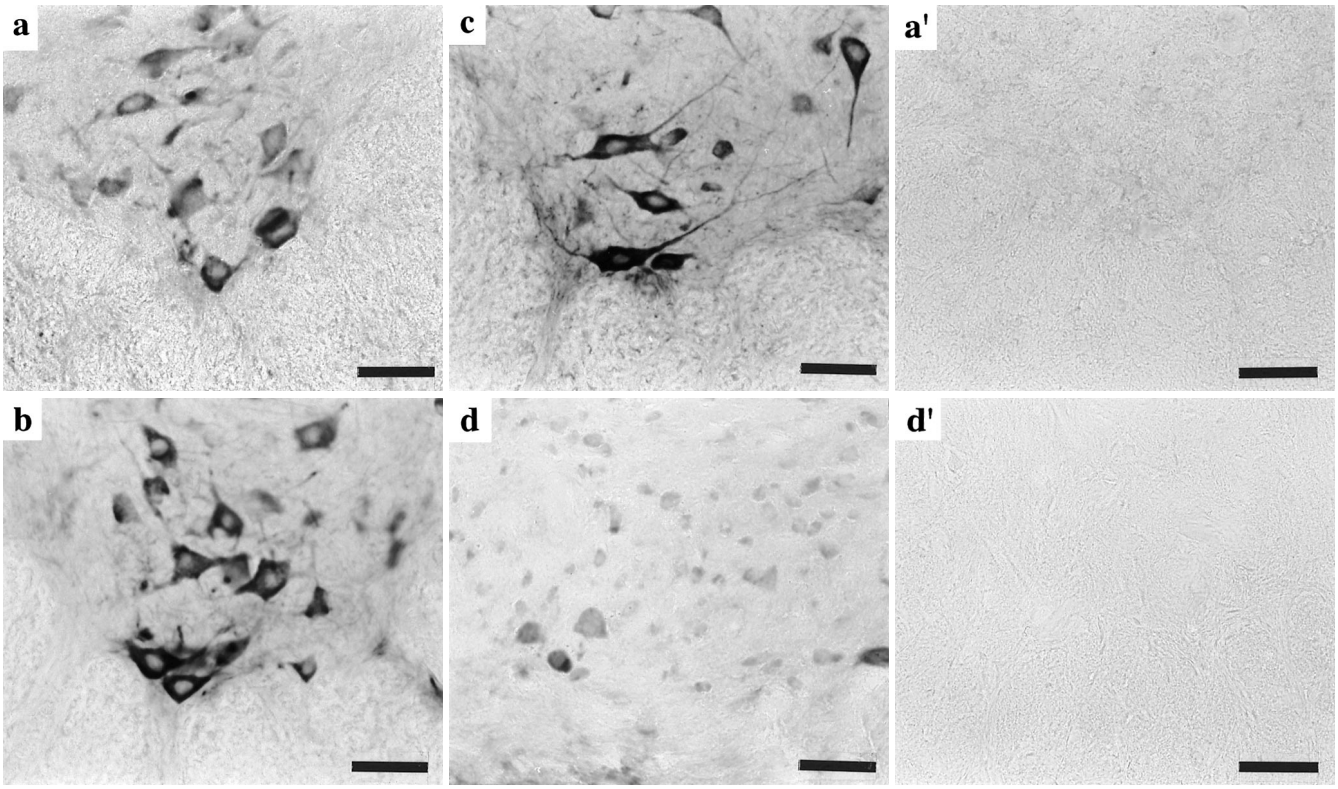

Fig. 5 Photomicrographs showing localisation of immunoreactivity of neurotrophin-3 in a representative control ICR mouse (**a**) and twy mouse with a transverse remnant area of 55% (**b–d**). **b** Site A; **c** site B; **d** site C. **a′**, **d′** Negative controls for ICR and twy mice, respectively. *Top* dorsal aspect of the cord. *Bar* 50 μm

site C (Fig. 5d), compared with that seen in ICR mice and also at sites A and B of twy mice.

Localisation of brain-derived neurotropic factor and neurotrophin-3 in the anterior white matter

BDNF and NT-3 immunoreactivity in the ICR and twy mice are shown in Fig. 6a–d. Severe compression (TRAS < 50%) was associated with increased BDNF immunoreactivity and abundant astroglia-like cells in the white matter at site B (Fig. 6b). A number of axons and nerve fibres at site B in the anterior columns also showed increased staining for anti-NT-3 V4 antibody compared with the posterior column, and they became coarse but had larger diameters, particularly at the exit of the ventral root (Fig. 6d), than in ICR mice.

Localisation of glial fibrillary acidic protein within the spinal cord

In control mice, type 1 and type 2 astrocytes were coarsely positive for GFAP in the white and grey matters, respectively (Fig. 7a). In the twy mouse with TRAS 70%, a number of astroglial cells were present entirely within the spinal cord, showing abundant nuclear chromatin, at and around the site of compression. In contrast, in twy mice with TRAS of 50–70%, astroglial cells strongly positive for GFAPs were significant at sites A (Fig. 7b), B (Fig. 7c), and C (Fig. 7d).

Topographic and quantitative analysis of brain-derived neurotropic factor and neurotrophin-3 immunoreactivity

A major band with a molecular weight of 17–19 kDa was commonly detected with anti-BDNF V4 antibody (Fig. 8a). Similarly, a band with a molecular weight of 30 kDa was detected with anti-NT-3 V4 antibody (Fig. 8b). In ICR mice, the relative ratios of density of BDNF and NT-3 V4 immunoreactivity in each band were 42–45% (*lanes 1, 2, 3, and 4* in Fig. 8a) and 49–51% (*lanes 1, 2, 3, and 4* in Fig. 8b), respectively. On the other hand, the relative ratios of BDNF and NT-3 V4 immunoreactivity at the compressed site (site C) were 26.3% (*lane 7* in Fig. 8a) and 39.0% (*lane 7* in Fig. 8b), respectively. Both ratios were significantly lower ($P < 0.05$) than those in ICR mice (*lane 3* in Figs. 8a and b). At site B in twy mice, BDNF V4 and NT-3 expression was 70.7% (*lane 6* in Fig. 8a) and 72.7% (*lane 6* in Fig. 8b), respectively ($P < 0.05$) when compared with that at site C). Similarly, immunoreactivity of both neu-

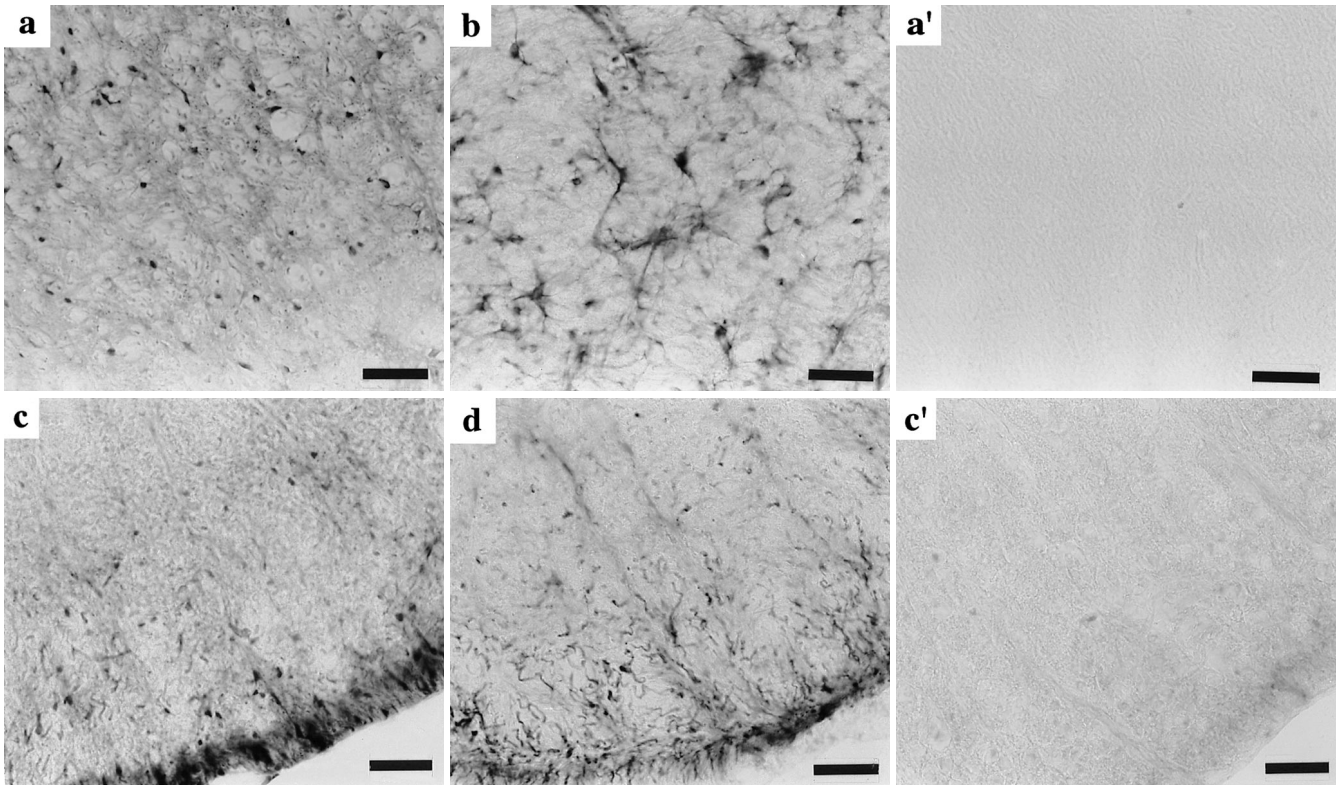

Fig. 6 Photomicrographs showing localisation of immunoreactivity of brain-derived neurotropic factor (BDNF) and neurotrophin (NT)-3 in the anterior column of the white matter in ICR and twy mice with a transverse remnant area of 30%, both at site B. **a**, **b** BDNF immunoreactivity in ICR and twy mice, respectively. **c**, **d** NT-3 immunoreactivity in ICR and twy mice, respectively. **a′**, **c′** Negative controls for BDNF and NT-3 in ICR mouse, respectively. *Bar* 50 μm

rotrophins increased significantly at the level distal to the compressed segment (*lane 8*).

Discussion

Using the twy mice, we have previously demonstrated a significant reduction in the number of anterior horn cells at the level of mechanical compression [4]. A progressively smaller number of these cells was noted when TRAS was 70% of the normal value, reaching an asymptote approximately below 50%. Hence, we postulated that TRAS of 70% could be regarded as the "threshold" level for survival of anterior horn cells at the level of compression. Interestingly, on the other hand, using the WGA-HRP-labelling method, we also found increased population of spinal accessory motoneurons at levels rostral to the C1 vertebra (sites free of direct mechanical compression) [7]. The latter finding led us to speculate that a group of motoneurons may translocate rostrally to avoid chronic mechanical compression. The present study was designed, therefore, to investigate the morphological behaviour and immunological reaction of the cervical spinal cord anterior horn cells under long-term traumatic compression. Our findings are particularly important when considering the neuronal reserve available for normal spinal cord function in the presence of mechanical injury.

The present study showed a small but insignificant decrease in the somal area and dendritic length at the site of compression (site C). It is generally believed that atrophy and reduced neuronal population occur when retrograde axonoplasmic transport is damaged in motoneurons of the central nervous system (CNS), although such an event allows some neuronal axons to regenerate and function at a later stage. Brännström et al. [10] demonstrated that permanent axonotomy in the adult cat causes a transient increase in the somal size of the spinal motoneuron followed by normalisation of the size, together with a decrease in the area of dendritic arborisation and the length of the neuron. Bowe et al. [9] described enlargement of the perikaryal area and thickening of dendrites without elongation of spinal motoneurons of mature rats following sciatic nerve crush injury. They suggested that the function of these neurons would subsequently decrease despite a certain degree of neuronal regeneration that may occur at a later stage.

Rostral to the site of mechanical compression (site B), we found enlargement of neuron soma and dendritic elongation of the WGA-HRP-labelled accessory motoneurons, which correlated significantly with deterioration of TRAS values measured at the site of compression. During devel-

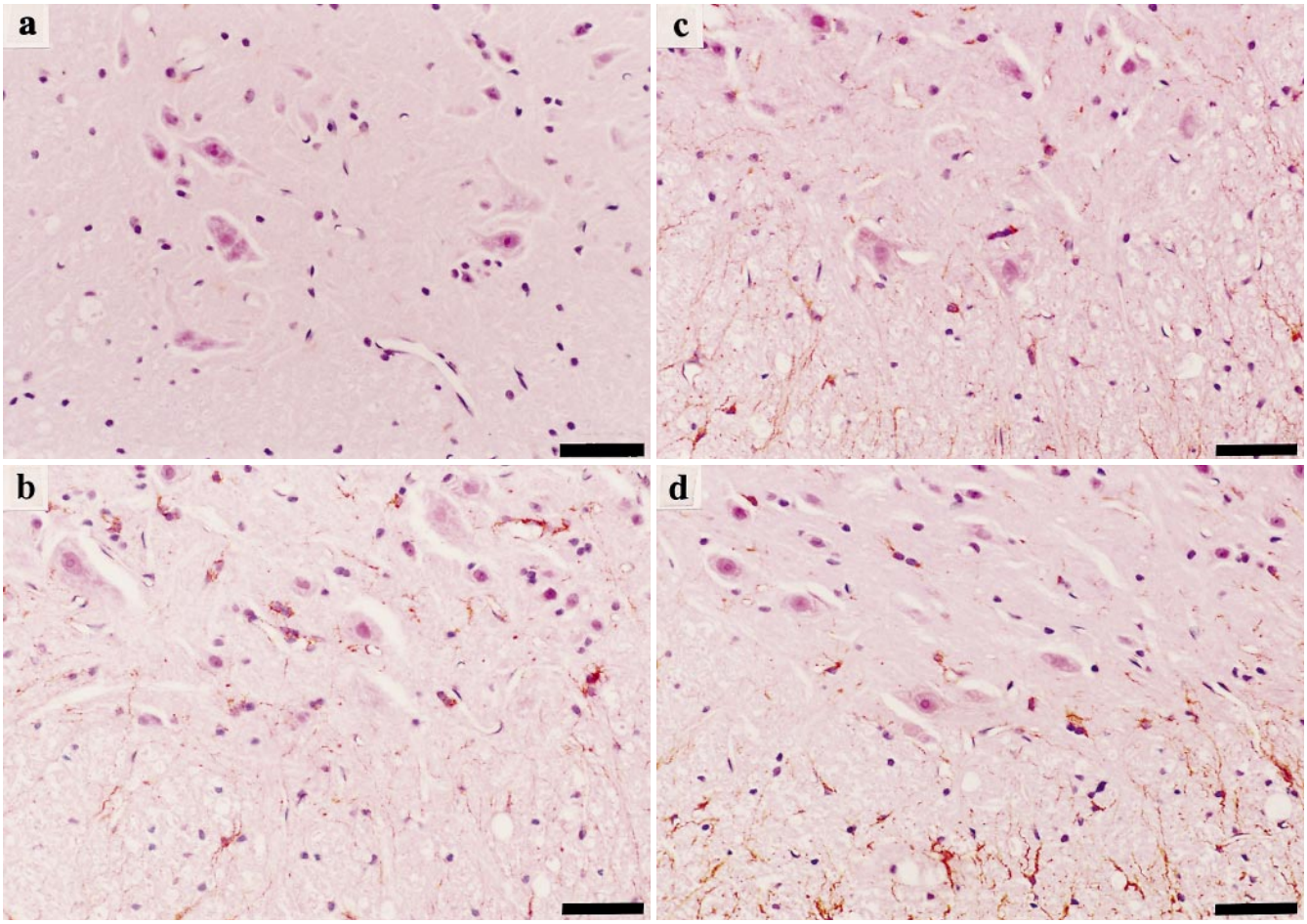

Fig. 7 Photomicrographs showing immunoreactivity of glial fibrillary acidic proteins in a representative ICR mouse (**a**) and a representative twy mouse with a transverse remnant area of 55% (**b–d**). **b** Site A; **c** site B; **d** site C. *Top* dorsal aspect of the cord. *Bar* 50 μm

opment of neuronal circuits, the neuron shows neurite growth towards the target areas followed by synaptic formation [35, 40]. Thus, during this process, the somal size and dendritic arborisation increase in order to facilitate synaptic connection [25]. In this regard, Purves and Lichtman [33] and Turner and Greenough [39] have indicated that increased dendritic density (arborisation) and formation of more complex synaptic networks represent enhanced synaptic circuits. Cullheim and Risling [12] observed regeneration of axons of cat lumbar motoneurons after intramedullary axonotomy, and identified the presence of vigorous neuronal activity aimed at regeneration of the neurons. On the other hand, O'Hanlon and Lowrie [32] demonstrated that 2–4 months after sciatic nerve crush injury, the neonatal rat spinal motoneuron showed enlargement of the soma and reorientation of dendrites with approximately 30% decrease in the total length of dendrites. In addition, using cholera toxin B-conjugated HRP, Goldstein et al. [19] showed that the morphology of dendrites of surviving spinal nucleus of the bulbocavernous following target deletion (extirpation of unilateral muscles) at birth could change, with significant increases in dendritic length and arborisation of dendrites. They also correlated dendritic reorganisation with possible influences of interaction of dendrites themselves. Our findings may represent enhancement of certain neuronal activities to compensate the compromised function of spinal cord motoneurons at the level of mechanical compression.

Nerve growth factors, such as BDNF and NT-3, act to promote the development of neurite outgrowth, growth and differentiation of neurons, as well as their survival [18, 22]. A number of reports [3, 8, 16, 29, 36, 38] have discussed the role of these and other factors in the CNS. Suzuki et al. [38] documented in hippocampal granular cells certain morphological changes of neurons after injection of kainate, including somatic as well as dendritic growth and increased nuclear volume. These changes correlated with overexpression of BDNF mRNA. Merlio et al. [29] also described increased expression of trkB mRNA, the receptor for BDNF and NT-3, following a variety of brain insults, and Arendt et al. [3] described reciprocal reactive expression of nerve growth factors following

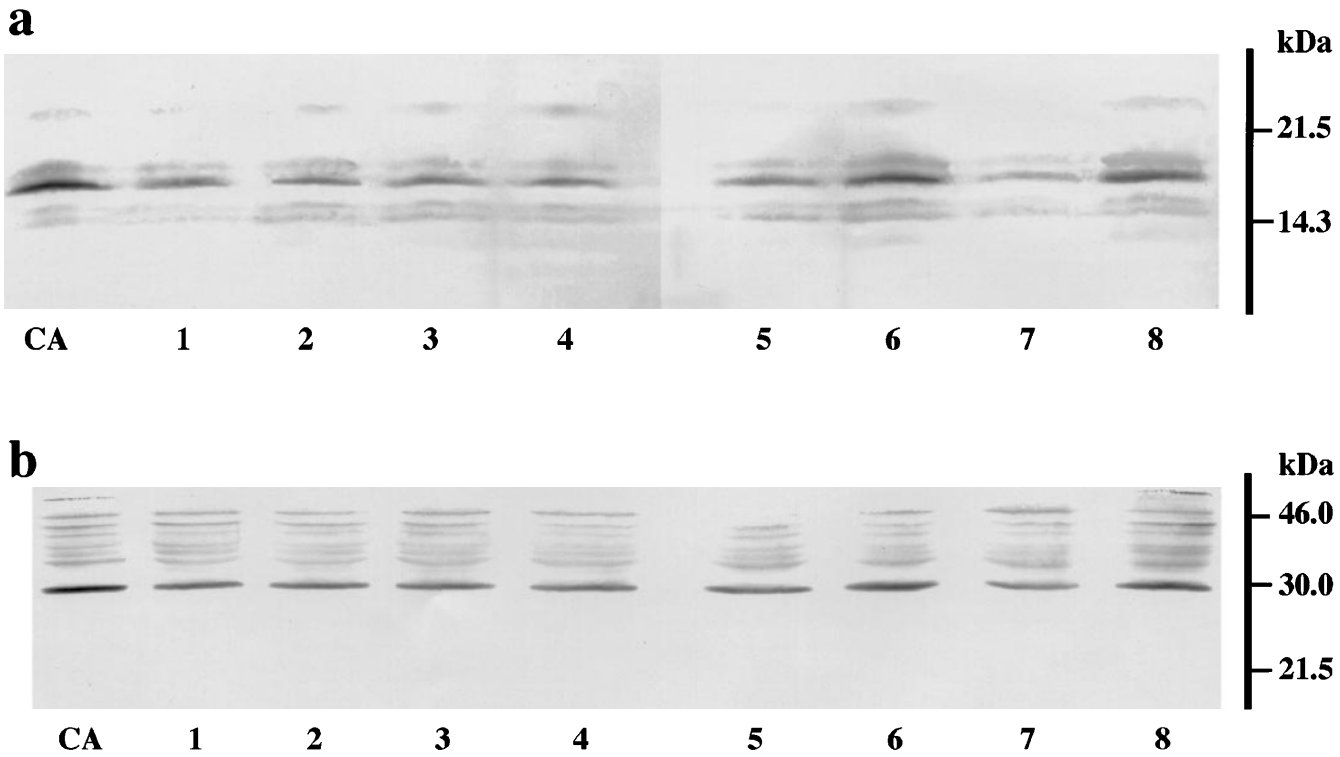

Fig. 8 Photomicrograph showing the expression of brain-derived neurotropic factor (**a**) and neurotrophin-3 (**b**) by Western blot analysis. The lane number shows each level of the spinal cord in the ICR (*lanes 1* to *4*) and twy (*lanes 5* to *8*) mice; *CA* refers to the hippocampus. *Lanes 1* and *5* site A, the level most rostral to the C1 ventral root; *lanes 2* and *6* site B, the level immediately rostral to compression between C1 ventral and C2 dorsal roots; *lanes 3* and *7* site C, between C2 and C3 dorsal roots (the compressed level in the twy mouse); *lanes 4* and *8* the level between C3 and C4 dorsal roots

chronic neurotoxic injury. Another important finding in our study was increased BDNF and NT-3 immunoreactivities in anterior horn cells, including spinal accessory motoneurons, in close association with increased neuronal density of motoneurons. In the spinal cord, Sendtner et al. [37] showed that BDNF and NT-3 effectively prevented the death of sciatic motoneurons in the newborn rat, and Yan et al. [42] reported that these neuropeptides prevented dysfunction of adult rat motoneurons (diminished activity of choline acetyltransferase) following axonotomy. In another experimental set-up, Schnell et al. [36] showed that NT-3 enhanced axonal growth and elongation of the injured rat corticospinal tract. Henderson et al. [20] showed that both polypeptides prevented death of cultured embryonic rat spinal cord motoneurons and mRNA within the neuron that encodes NT-3. In the present study, we found a significantly weak immunostaining for both BDNF and NT-3 V4 antibodies in anterior horn cells located at the level of severe compression (site C), while at levels rostral to the compression (site B), an overexpression of these neuropeptides was detected in anterior horn cells, when TRAS ranged between 50% and 70%. Thus, the presence of severe mechanical compression was associated with a marked increase in immunoreactivity of these neuropeptides. Furthermore, heterotropically translocated motoneurons showed increased activities of BDNF and NT3 together with enlargement of the soma and dendritic elongation associated with extensive arborisation of dendrites. We speculate that for an effective utilisation of these neuropeptides, these neurons may have a particular autocrine mechanism, as suggested by Fukumitsu et al. [17]. Furthermore, since motoneurons express trkB and trkC mRNAs [18], it is possible that the uptake of BDNFs occurs in tissues other than neurons themselves. Interestingly, the expression of NT-3 was more significant in the ventral region of the anterior column (Fig. 6d). In newborn and adult rats, nerve growth factors are produced not only by neurons and Schwann cells but also by fibroblasts of their targets as well [42]. We postulate that considerable amounts of neuropeptides are transported retrogradely [13, 27, 43] and/or from the brain [15], in order to increase neuronal activity as well as axonal transport.

It is generally believed that reactive astrocytosis (infiltration of astroglial cells) followed by some scar tissue formation occur following injury of the CNS, including the spinal cord. Reactive astrogliosis may inhibit regeneration of axons as well as dendrites [21, 34]. In the twy mouse, histological evidence of significant oedema, necrosis, cystic formation and fibrous scar formation is usually absent, while atrophy and loss of neurons are

noted at levels proportionate to the extent of compression. In the twy mouse, reactive astrocytosis was significant at sites other than the level of compression. It is known that astroglial cells produce BDNF [8] and other nerve growth factors [26]. In the spinal cord injury model, Frisén et al. [16] demonstrated that trkB mRNA, the receptor for BDNF, is strongly positive in motoneurons and astroglial cells, and axonal regeneration was more marked at the site with significant increase in trkB mRNA immunoreactivity within the white matter. In the present study, when TRAS was 55% of the control, a number of infiltrated astroglial cells, positive for BDNF immunostaining, were detected at sites rostral to the site of compression, particularly in the white matter, where an increased number of motoneurons was noted. Based on these findings, we postulate that reactive astroglial cells in twy mice with severe spinal cord compression produce BDNF, which enhances neuronal repair and regeneration.

In conclusion, we used the twy mouse, which simulates spondylosis and ossified posterior longitudinal ligament, in order to elucidate topographically the mechanisms of neuronal changes in chronic spinal cord compression. WGA-HRP-labelled accessory motoneurons were found to express significant BDNF and NT-3 immunoreactivities that correlated with enlargement of neuronal soma and extensive dendritic arborisation at levels rostral to the site of mechanical compression. Heterotropically infiltrated astroglial cells at these levels may play an important role in neuronal reserve and survival and probably the production of such neurotropic factors.

Acknowledgements This work was supported in part by a grant from the Investigation Committee on Ossification of the Spinal Ligaments, the Public Health Bureau of the Ministry of Health and Welfare of the Japanese Government (1996) and a Grant-in-Aid for General Scientific Research of the Ministry of Education, Science and Culture of Japan (grant no. 09671480).

References

1. Albers FJ, Meek J (1991) Dendritic and synaptic properties of collicular neurons: a quantitative light and electron microscopical study of Golgi-impregnated cells. Anat Rec 231:524–537
2. Al-Mefty O, Harkey HL, Marawi I (1993) Experimental chronic compressive myelopathy. J Neurosurg 79:550–561
3. Arendt T, Brückner MK, Pagliusi S, Krell T (1995) Degeneration of rat cholinergic basal forebrain neurons and reactive changes in nerve growth factor expression after chronic neurotoxic injury. I. Degeneration and plastic response of basal forebrain neurons. Neuroscience 65:633–645
4. Baba H, Maezawa Y, Imura S, Kawahara N, Nakahashi K, Tomita K (1996) Quantitative analysis of the spinal cord motoneuron under chronic compression: an experimental observation in the mouse. J Neurol 243:109–116
5. Baba H, Uchida K, Maezawa Y, Furusawa N, Azuchi M, Imura S (1996) Lordotic alignment and posterior migration of the spinal cord following en bloc open-door laminoplasty for cervical myelopathy: a magnetic resonance imaging study. J Neurol 243:626–632
6. Baba H, Maezawa Y, Uchida K, Furusawa N, Wada M, Imura S (1997) Plasticity of the spinal cord contributes to neurological improvement in patients treated by cervical decompressive surgery: a magnetic resonance imaging study. J Neurol 244:455–460
7. Baba H, Maezawa Y, Uchida K, Imura S, Kawahara N, Tomita K, Kudo M (1997) Three-dimensional topographic analysis of spinal accessory motoneurons under chronic mechanical compression: an experimental study in the mouse. J Neurol 244:222–229
8. Barde Y-A, Edgar D, Thoenen H (1982) Purification of a new neurotropic factor from mammalian brain. EMBO J 1:549–553
9. Bowe CM, Evance NH, Vlacha V (1992) Progressive morphological abnormalities observed in rat spinal motor neurons at extended intervals after axonal regeneration. J Comp Neurol 321:576–590
10. Brännström T, Havton L, Kellerth J (1992) Changes in size and dendritic arborization patterns of adult cat spinal motoneurons following permanent axonotomy. J Comp Neurol 318:439–451
11. Claiborne BJ, Amaral DG, Cowan WM (1990) Quantitative, three-dimensional analysis of granule cell dendrites in the rat dentate gyrus. J Comp Neurol 302: 206–219
12. Cullheim S, Risling M (1992) A light and electron microscopic study of intracellularly HRP-labeled lumbar motoneurons after intramedullary axonotomy in the adult cat. J Comp Neurol 318:188–208
13. Di Stefano PS, Friedman B, Radziejewski C, Alexander C, Boland P, Schick CM, Lindsay RM, Wiegand SJ (1992) The neurotrophins BDNF, NT-3, and NGF display distinct patterns of retrograde axonal transport in peripheral and central neurons. Neuron 8: 983–993
14. Eng LF (1980) The glial fibrillary acidic (GFA) protein. In: Bradshaw RA, Schneider DM (eds) Proteins of the nervous system. Raven Press, New York, pp 85–117
15. Ernfos P, Persson H (1991) Developmentally regulated expression of HDNF/NT-3 mRNA in rat spinal cord motoneurons and expression of BDNF mRNA in embryonic dorsal root ganglion. Eur J Neurosci 3:953–961
16. Frisén J, Verge VMK, Cullheim S, Persson H, Fried K, Middlemas DS, Hunter T, Hökfelt T, Risling M (1992) Increased levels of trkB mRNA and trkB protein-like immunoreactivity in the injured rat and cat spinal cord. Proc Natl Acad Sci USA 89:11282–11286
17. Fukumitsu H, Furukawa Y, Tsusaka M, Kinukawa H, Nitta A, Nomoto H, Mima T, Furukawa S (1998) Simultaneous expression of brain-derived neurotropic factor and neurotrophin-3 in Cajal-Retzius, subplate and ventricular progenitor cells during early developmental stages of the rat cerebral cortex. Neuroscience (in press)
18. Funakoshi H, Frisén J, Barbany G, Timmusk T, Zachrisson O, Verge V, Persson H (1993) Differential expression of mRNA for neurotrophins and their receptors after axonotomy of the sciatic nerve. J Cell Biol 123:455–465
19. Goldstein LA, Kurtz EM, Kalkbrenner AE, Sengelaub DR (1993) Changes in dendritic morphology of rat spinal motoneurons during development and after unilateral target deletion. Dev Brain Res 73:151–163

20. Henderson CE, Camu W, Mettling C, Gouin A, Poulsen K, Karihaloo M, Rullamas J, Evans T, McMahon SB, Armanini MP, Berkemeier L, Phillips HS, Rosenthal A (1993) Neurotrophins promote motor neuron survival and are present in embryonic limb bud. Nature 363:266–270
21. Ikuta F (1991) The process of brain lesion repair and activity of astrocytes. In: Ikuta F (ed) Neuropathology in brain research. Elsevier, Amsterdam, pp 211–231
22. Johnson EM, Taniuchi M, DeStefano PS (1988) Expression and possible function of nerve growth factor receptors on Schwann cells. Trends Neurosci 11:299–304
23. Kameyama T, Hashizume Y, Ando T, Takahashi A, Yanagi T, Mizuno J (1995) Spinal cord morphology and pathology in ossification of the posterior longitudinal ligament. Brain 118:263–278
24. Kitamura S, Sakai A (1982) A study on the localization of the sternocleidomastoid and trapezius motoneurons in the rat by means of the HRP method. Anat Rec 202:527–536
25. Kozio JA, Tuckwell HC (1978) Analysis and estimation of synaptic dendrites and their spatial variation on the motoneuron surface. Brain Res 150:617–624
26. Lu B, Yokoyama M, Dreyfus CF, Black IB (1991) NGF gene expression in active growing brain glia. J Neurosci 11:318–326
27. Maisonpierre PC, Belluscio L, Friedman B, Alderson RF, Wiegand SJ, Furth ME, Lindsay RM, Yancopoulos GD (1990) NT-3, BDNF, and NGF in the developing rat nervous system: parallel as well as reciprocal patterns of expression. Neuron 5:501–509
28. Martin D, Schoenen J, Delrée P, Gilson V, Rogister B, Leprince P, Stevenaert A, Moonen G (1992) Experimental acute traumatic injury of adult rat spinal cord by a subdural inflatable balloon: methodology, behavioral analysis, and histopathology. J Neurosci Res 32:539–550
29. Merlio JP, Ernfors P, Kokaia Z, Middlemas DS, Bengzon J, Kokaia M, Smith MJ, Siesjo BK, Hunter T, Lindvall O, Persson H (1993) Increased production of trkB protein tyrosine kinase receptor after brain insults. Neuron 10:151–164
30. Mesulam MM (1978) Tetramethylbenzidine for horseradish peroxidase neurohistochemistry: a non-carcinogenic blue reaction-product with superior sensitivity for visualizing neural afferents and efferents. J Histochem Cytochem 26:106–117
31. Mizuno J, Nakagawa H, Iwata K, Hashizume Y (1992) Pathology of spinal cord lesions caused by ossification of the posterior longitudinal ligament, with special reference to reversibility of the spinal cord lesion. Neurol Res 14:312–314
32. O'Hanlon GM, Lowrie MB (1993) Neonatal nerve injury causes long-term changes in growth and distribution of motoneuron dendrites in the rat. Neuroscience 56:453–464
33. Purves D, Lichtman JW (1985) Geometrical differences among homologous neurons in mammals. Science 228:298–302
34. Reiter PJ, Stennas LJ, Guth L (1983) The astrocytic scar as an impediment to regeneration in the central nervous system. In: Kao CC, Burge RP, Reiter PJ (eds) Spinal cord reconstruction. Raven Press, New York, pp 163–208
35. Richardson PM, McGuinnes UM, Aguayo AJ (1980) Axons from CNS neuron regenerate into PNS grafts. Nature 284:264–265
36. Schnell L, Schneider R, Kolbeck R, Barde Y-A, Schwab ME (1992) Neurotrophin-3 enhances sprouting of corticospinal tract during development and after adult spinal cord lesion. Nature 367:170–173
37. Sendtner M, Holtmann B, Kolbeck R, Thoenen H, Barde Y-A (1992) Brain-derived neurotropic factor prevents death of motoneurons in newborn rats after nerve section. Nature 360:170–173
38. Suzuki F, Junier M-P, Guilheim D, Sørensen J-C, Onteniente B (1995) Morphogenetic effect of kainate on adult hippocampal neurons associated with a prolonged expression of brain-derived neurotropic factor. Neuroscience 64:665–674
39. Turner AM, Greenough WT (1985) Differential rearing effect on rat visual cortex synapses per neuron. Brain Res 329:195–203
40. Vidal-Sanz M, Bray GM, Villegas-Perez MP, Thanos S, Aguayo A (1987) Axonal regeneration and synapse formation in the superior colliculus by retinal ganglion cells in the adult rat. J Neurosci 7:2894–2909
41. Yamamoto T, Noda T, Oka H, Yoshida K, Tamamaki N (1989) Three-dimensional computer-aided reconstruction of non-pyramidal neurons in the cat primary somatosensory cortex. Neurosci Res 9 [Suppl]: S166
42. Yan Q, Elliot JL, Matheson C, Sun J, Zhang L, Mu X, Rex KL, Snider WD (1993) Influences of neurotrophins on mammalian motoneurons in vivo. J Neurobiol 24:1555–1577
43. Zhou X-F, Rush RA (1993) Localization of neurotrophin-3-like immunoreactivity in peripheral tissues of the rat. Brain Res 621:189–199